

## Article

# Optimization of Ammonia Nitrogen Removal and Recovery from Raw Liquid Dairy Manure Using Vacuum Thermal Stripping and Acid Absorption Process: A Modeling Approach Using Response Surface Methodology

Srijana Sapkota <sup>1</sup>, Arif Reza <sup>2,3</sup> and Lide Chen <sup>4,\*</sup>

<sup>1</sup> Environmental Science Program, College of Natural Resources, University of Idaho, Moscow, ID 83844, USA; ssapkota@uidaho.edu

<sup>2</sup> NYS Center for Clean Water Technology, Stony Brook University, Stony Brook, NY 11794, USA; arif.reza@stonybrook.edu

<sup>3</sup> School of Marine and Atmospheric Sciences, Stony Brook University, Stony Brook, NY 11794, USA

<sup>4</sup> Department of Soil and Water Systems, Twin Falls Research and Extension Center, University of Idaho, 315 Fall Avenue East, Twin Falls, ID 83303, USA

\* Correspondence: lchen@uidaho.edu

**Abstract:** Dairy manure adds a substantial amount of nitrogen to wastewater due to its high levels of associated nutrients. Removal and recovery of ammonia nitrogen (NH<sub>3</sub>-N) from raw liquid dairy manure (RLDM) is greatly valued. This study was focused on the vacuum thermal stripping–acid absorption (VTS-AA) process for NH<sub>3</sub>-N from RLDM, followed by modeling and optimization. Using the response surface methodology (RSM)-based central composite design (CCD) approach, the critical operational parameters of the vacuum thermal stripping process, including temperature (50–70 °C), pH (9–11), vacuum pressure (35–55 kPa), and treatment time (60–90 min), were optimized. With the specified parameters set at temperature 69.9 °C, pH 10.5, vacuum pressure 53.5 kPa, and treatment time 64.2 min, the NH<sub>3</sub>-N removal efficiency attained was 98.58 ± 1.05%, aligning closely with the model prediction. Furthermore, the recovered ammonium sulfate ((NH<sub>4</sub>)<sub>2</sub>SO<sub>4</sub>) closely matched their commercial counterparts, confirming the effectiveness of the VTS-AA process in recovering NH<sub>3</sub>-N from RLDM. The distinct advantage of the employed technology lies in the concurrent energy demand reduction achieved by introducing a vacuum system. These findings contribute valuable insights into the practical implementation of the VTS-AA process for treating raw dairy manure, particularly in large-scale operational contexts.

**Keywords:** ammonia removal and recovery; raw liquid dairy manure; vacuum thermal stripping; optimization; response surface methodology; central composite design



**Citation:** Sapkota, S.; Reza, A.; Chen, L. Optimization of Ammonia Nitrogen Removal and Recovery from Raw Liquid Dairy Manure Using Vacuum Thermal Stripping and Acid Absorption Process: A Modeling Approach Using Response Surface Methodology. *Nitrogen* **2024**, *5*, 409–425. <https://doi.org/10.3390/nitrogen5020026>

Academic Editor: Shuguang Deng

Received: 15 March 2024

Revised: 30 April 2024

Accepted: 7 May 2024

Published: 9 May 2024



**Copyright:** © 2024 by the authors. Licensee MDPI, Basel, Switzerland. This article is an open access article distributed under the terms and conditions of the Creative Commons Attribution (CC BY) license (<https://creativecommons.org/licenses/by/4.0/>).

## 1. Introduction

Livestock production in the United States has increased substantially since the 1970s, resulting in a notable rise in the volume of wastewater generated from these operations [1]. An estimated millions of tons of livestock manure were produced annually in the United States (US) alone [2]. Dairy manure is characterized by high levels of dissolved and suspended solids, incorporating fats, oils, and grease. Additionally, it contains nutrients like ammonia and phosphates, along with high levels of biochemical oxygen demand (BOD) and chemical oxygen demand (COD) [3]. Raw liquid dairy manure (RLDM) is characterized by high ammonia (NH<sub>3</sub>) concentrations. Ammonia is known for its adverse environmental effects and the potential harm it may cause to aquatic ecosystems. As dairy manure production increases, there is a crucial need for a system that can efficiently extract its nutrient content without causing harmful pollution in the air, soil, or water [4]. In both digested and undigested forms of dairy manure, ammonia has been identified as

the predominant pollutant, existing in the forms of free ammonia ( $\text{NH}_3$ ) and ammonium ( $\text{NH}_4^+$ ) [5]. The liquid manure derived from barns, which has not undergone digestion, might introduce difficulties in manure management as  $\text{NH}_3$  concentrations reach as high as 936 mg/L [6]. As per the Environmental Protection Agency (EPA),  $\text{NH}_3$  emissions from animal production facilities in the United States were approximately 3.2 million tons in 2002, with a projection indicating an increase to 3.8 million tons by 2030 (USEPA, 2004). Ammonia removal and recovery from wastewater have become central issues on a global scale, representing essential steps towards establishing a sustainable nitrogen cycle and circular economy [7].

Industry operators find effective wastewater treatment increasingly challenging, particularly with the stringent discharge standards enforced by regulatory bodies and pollution control boards [8]. The conventional treatment methods for industrial and municipal wastewater may exceed individual dairy farmer's financial and technical capabilities [9]. The feasibility of treating dairy manure using conventional wastewater treatment processes is likely to be compromised due to manure characteristics like high solids content [9]. Additionally, the effectiveness of the biological nitrogen removal process may be compromised by the excessive presence of  $\text{NH}_3\text{-N}$  and other harmful compounds [10]. Unlike municipal and industrial wastewater, dairy liquid manure is generated intermittently, so a batch-operating system is necessary for effective  $\text{NH}_3\text{-N}$  removal [5].

Ammonia nitrogen ( $\text{NH}_3\text{-N}$ ) from dairy manure has been removed using technologies such as coupled air- or steam-stripping and acid absorption [9,11,12], struvite precipitation [13,14], and membrane distillation [15]. Gas stripping has some concerns regarding cost and system modelling [16]. The struvite recovery technologies mainly prioritize phosphate recovery with a small reduction in  $\text{NH}_3$ , often under 30% [17]. However, the findings from this research have yet to be widely implemented on an industrial scale due to diverse factors such as technical challenges, economic constraints, complex operation, or maintenance requirements [15,18]. Ukwuani and Tao [19] first developed and employed vacuum thermal stripping–acid absorption (VTS-AA) for  $\text{NH}_3$  recovery from anaerobically digested liquid dairy manure both at the lab and pilot scale and found it to be an effective and cost-effective method for efficiently recovering ammonia from dairy wastewater. They observed that over 93% of  $\text{NH}_3$  was successfully removed through the vacuum stripping process from dairy manure digestate in 3 h. Recently, Reza and Chen [20] further improved and optimized the VTS-AA process to make the technology more efficient. They studied the impact of boiling point temperature, vacuum, and treatment time on the stripping and absorption of  $\text{NH}_3\text{-N}$  in anaerobically digested liquid dairy manure. Their findings suggested that at 70 °C and 44 kPa, over 93% of  $\text{NH}_3\text{-N}$  could be stripped within 1.5 h. Similarly, to examine how different parameters influence efficiency and mass transfer, Chen et al. [21] conducted five sets of temperature and vacuum pressure combinations for vacuum ammonia stripping of sludge digestate: 53 °C at 15 kPa, 60 °C at 20 kPa, 65 °C at 25 kPa, 72 °C at 35 kPa, and 81 °C at 50 kPa. The findings revealed that 80% of  $\text{NH}_3\text{-N}$  was removed within 45 min across all experimental groups. During the VTS-AA process, the aqueous  $\text{NH}_4^+$  in wastewater is converted to free  $\text{NH}_3$  at a temperature lower than the average boiling point. In this setting,  $\text{NH}_3$  is successfully evaporated from the stripping chamber, then absorbed into an acid solution (commonly sulfuric acid,  $\text{H}_2\text{SO}_4$ ) aided by the vacuum, yielding ammonium sulfate crystals [19,22]. Vacuum thermal stripping takes advantage of the lower boiling point and higher vapor pressure of  $\text{NH}_3$  relative to water, thus minimizing water evaporation associated with distillation and subsequently reducing energy consumption [23]. This method, therefore, possess remarkable  $\text{NH}_3$  removal capabilities, along with higher and more effective recovery potential. VTS-AA treatment maintains the advantage of the traditional air-stripping treatment by recycling the removed  $\text{NH}_3\text{-N}$  as ammonium sulfate ( $(\text{NH}_4)_2\text{SO}_4$ ) crystals, a marketable fertilizer product. Without the input of fertilizer nitrogen, it is estimated that only about half of the current global population can be supplied with sufficient food energy and protein [24].

To date, anaerobically digested waste streams are mostly used for NH<sub>3</sub>-N recovery in VTS-AA studies, which leaves a significant gap in raw wastewater research such as raw liquid dairy manure (RLDM), mainly because of its lower nitrogen concentrations [19,20,25]. Existing studies have highlighted the influence of diverse factors, including pH, temperature, treatment duration, vacuum pressure, and concentration, on ammonia removal from processed wastewater during the laboratory exploration stages [21,26–28]. A comprehensive understanding of the impact of operational parameters on a VTS-AA unit and the distinctive characteristics of RLDM that contribute to NH<sub>3</sub>-N removal and recovery is imperative. Hence, this study was focused on optimizing and investigating the impact of key operational parameters (viz. temperature, pH, vacuum pressure, and treatment time) for efficient NH<sub>3</sub>-N removal and recovery from RLDM via employing a response surface methodology (RSM)-based central composite design (CCD) model.

## 2. Materials and Methods

### 2.1. Sample Collection and Characterization

Centrifuged RLDM samples were collected from a commercial dairy in Southern Idaho’s Magic Valley region and subsequently filtered using a ten-mesh (2000 µm) sieve at the Twin Falls Research and Extension Center of University Idaho to discard extra fibers and solid residues. The resulting feed samples were stored at 4 °C until experimental use.

The physicochemical properties of the collected RLDM are shown in Table 1.

**Table 1.** Characteristics of the collected raw liquid dairy manure.

Characteristics	Average ± Standard Deviation
Total Solid (TS) (%)	2.71 ± 0.01
Suspended Solid (TSS) (%)	0.93 ± 0.05
Dissolved Solid (TDS) (%)	1.78 ± 0.04
Chemical Oxygen Demand (COD) (mg/L)	25,120 ± 677.97
Total Phosphorus (TP) (mg/L)	741 ± 12.49
Orthophosphate (OP) (mg/L)	406.3 ± 9.07
Ammonia Nitrogen (NH <sub>3</sub> -N) (mg/L)	562.1 ± 13.10
Nitrate Nitrogen (NO <sub>3</sub> -N) (mg/L)	51.2 ± 0.48
Nitrite Nitrogen (NO <sub>2</sub> -N) (mg/L)	5.1 ± 0.40
Total Kjeldahl Nitrogen (TKN) (mg/L)	1109.3 ± 109.64
Total Nitrogen (TN) (mg/L)	1436.7 ± 106.81
pH	7.04 ± 0.06

### 2.2. Vacuum Thermal Stripping–Acid Absorption Setup and Experimental Procedure

In our previous study, a VTS-AA lab-scale experimental setup was designed and developed to remove and recover NH<sub>3</sub>-N from anaerobically digested liquid dairy manure (ADLDM) [20]. In this study, the same experimental setup was repurposed to investigate NH<sub>3</sub>-N removal and recovery from RLDM, incorporating pH as one of the four key operational parameters. This adjustment allowed us to analyze the impact of varying pH levels on the NH<sub>3</sub>-N removal and recovery within the VTS-AA process. Such a streamlined approach not only enhanced VTS process performance but also allowed us to scrutinize deeper into a new research question without the need for further modifications. The continuity in the experimental setup helped ensure consistency in methodology.

The experimental setup for NH<sub>3</sub>-N removal and recovery from RLDM involved a 500 mL three-neck round bottom flask with a magnetic stirrer operating at 150 rpm to ensure thorough sample mixing. Precise control was achieved by integrating essential instruments, including a vacuum gauge, heating mantle, temperature controller, and thermometer. In each batch of the NH<sub>3</sub>-N removal and recovery experiment, 75 mL of RLDM was introduced into the flask, and heated using a 270 W lower hemispherical cloth heating mantle which was connected to a digital bench-top temperature controller. The details of the experimental setup can be obtained from the earlier study [20].

Three sets of batch experiments were conducted to assess the impact of critical operating parameters on VTS-AA treatment from RLDM. Feed samples of 1 mL were collected before and after each experiment and analyzed for NH<sub>3</sub>-N concentration.

The response variable in this study is the percentage of NH<sub>3</sub>-N removed (%) from RLDM, calculated using the formula below:

$$\text{Removal Efficiency(\%)} = \frac{(C_0 - C_t)}{C_0} \times 100 \quad (1)$$

where  $C_0$  is the initial NH<sub>3</sub>-N concentration (mg/L) and  $C_t$  is the final NH<sub>3</sub>-N concentration (mg/L) at treatment time  $t$ .

### 2.3. Experimental Design

The RSM-based CCD was adopted as the experimental design in this study. Four influential operational parameters, specifically temperature, pH, vacuum pressure, and treatment time for NH<sub>3</sub>-N removal and recovery from RLDM, were optimized. As a robust experimental design, CCD helps optimize the process performance and analyze interactions among the parameters with a minimal number of experiments [29]. Moreover, it simplifies the understanding of orthogonal blocking and rotatability, the critical aspects of process optimization [30]. For a 4-factor CCD design, the total number of experimental runs was calculated using the following Equation (2):

$$N = 2^k + 2k + c \quad (2)$$

where  $N$  is the number of experiments,  $k$  is the number of factors, and  $c$  is the number of central points.

Based on the above equation, 30 experiments, including 16 factorial, 8 axial, and 6 replications of central points, were performed in this study. The order of these experimental runs was randomized to minimize bias and account for any potential external factors that could influence the results.

The levels of the four study parameters were determined based on preliminary studies and a literature review to ensure a wide range of conditions [20,27,31]. Each experiment was conducted in triplicate, and the data analysis relied on the average experimental observation values. In the experimental procedure, RSM used second-order polynomial regression to approximate the fitting of a mathematical model. This method assessed the effects of multiple parameters and their interactions in this study. The four parameters, namely temperature, pH, vacuum pressure, and treatment time, were denoted as  $A$ ,  $B$ ,  $C$ , and  $D$ , respectively. The experimental data obtained from the CCD runs were subjected to statistical analysis using Design-Expert<sup>®</sup> software (version 13.0.5, StatEase, Inc., Minneapolis, MI, USA).

The predictive model for this study was formulated as a second-order regression (Equation (3)).

$$Y = \beta_0 + \beta_1 A + \beta_2 B + \beta_3 C + \beta_4 D + \beta_{12} AB + \beta_{13} AC + \beta_{14} AD + \beta_{23} BC + \beta_{24} BD + \beta_{34} CD + \beta_{11} A^2 + \beta_{22} B^2 + \beta_{33} C^2 + \beta_{44} D^2 \quad (3)$$

where  $Y$  is the predicted response directly related to the NH<sub>3</sub>-N removal efficiency,  $A$ ,  $B$ ,  $C$ , and  $D$  are the independent variables,  $\beta_0$  implies intercept,  $\beta_1$ ,  $\beta_2$ ,  $\beta_3$ , and  $\beta_4$  represent linear coefficients,  $\beta_{11}$ ,  $\beta_{22}$ ,  $\beta_{33}$ , and  $\beta_{44}$  represent quadratic coefficients, and  $\beta_{12}$ ,  $\beta_{13}$ ,  $\beta_{14}$ ,  $\beta_{23}$ ,  $\beta_{24}$ , and  $\beta_{34}$  constitute the interaction coefficients.

The statistical significance of the model and its individual terms, including main effects and interactions, was evaluated using analysis of variance (ANOVA). Three-dimensional surface and contour plots were utilized to visually demonstrate the interactions and impact of the independent parameters on the target response. Table 2 displays the independent factors along with their coded and real values.

**Table 2.** Values of the selected independent parameters tested in the RSM.

Parameters	Coded/Real Values		
	−1	0	+1
Temperature (A) (°C)	50	60	70
pH (B)	9	10	11
Vacuum pressure (C) (kPa)	35	45	55
Treatment time (D) (Min)	60	75	90
Rotation speed (rpm)		150	

The coded form of three different levels for each experiment are −1, 0, +1. In this way, the coded variables are within −1 (minimum value) and +1 (maximum value) [32].

#### 2.4. Process Optimization and NH<sub>3</sub>-N Recovery Process

Using the described experimental setup, process optimization datasets were generated. Three VTS-AA tests were carried out under optimized conditions to assess the model's predictive accuracy. Following this, the resulting solutions, which contained absorbed NH<sub>3</sub>-N and a saturated solution of 100 mL H<sub>2</sub>SO<sub>4</sub> (2N), went through a process of crystallization. The crystals formed were improved by storing them at 4 °C for 24 h. Thereafter, these three solutions were subjected to vacuum filtration using Buchner flask to separate the acidic solution from the crystallized ammonium sulfate ((NH<sub>4</sub>)<sub>2</sub>SO<sub>4</sub>). The collected crystals were then dried in a laboratory oven at 100 °C for 4–5 h. Ultimately, three sets of collected (NH<sub>4</sub>)<sub>2</sub>SO<sub>4</sub> crystals were sent to the Electron Microscopy Center at the University of Idaho for SEM and XRD analyses.

### 3. Results and Discussion

#### 3.1. Ammonia Nitrogen Removal from RLDM: Model Fitting and Data Analysis

The second-order polynomial quadratic equation of the NH<sub>3</sub>-N removal was developed based on the obtained data in coded form through RSM:

$$\begin{aligned} \text{NH}_3\text{-N Removal efficiency (\%)} = & 89.43 + 6.85A + 6.86B + 3.42C + 2.85D + \\ & 2.47A^2 - 5.32B^2 - 0.1785C^2 + 0.2515D^2 - 4.19AB - 0.78AC - 0.0956AD - \\ & 1.12BC - 1.29BD - 0.7169CD \end{aligned} \quad (4)$$

Results obtained from the VTS-AA using the CCD matrix are shown in Table 3.

**Table 3.** Experimental design with experimental and predicted responses of independent variables.

S. N	Independent Parameters <sup>(1)</sup>				Response (Y): NH <sub>3</sub> -N Removal Efficiency (%)	
	A (°C)	B	C (kPa)	D (Min)	Experimental Value	Predicted Value
1	50 (−1)	9 (−1)	35 (−1)	60 (−1)	59.77	58.49
2	70 (+1)	9 (−1)	35 (−1)	60 (−1)	81.62	82.32
3	50 (−1)	11 (+1)	35 (−1)	60 (−1)	84.88	85.39
4	70 (+1)	11 (+1)	35 (−1)	60 (−1)	93.22	92.48
5	50 (−1)	9 (−1)	55 (+1)	60 (−1)	69.99	70.56
6	70 (+1)	9 (−1)	55 (+1)	60 (−1)	92.98	91.25
7	50 (−1)	11 (+1)	55 (+1)	60 (−1)	93.59	92.98
8	70 (+1)	11 (+1)	55 (+1)	60 (−1)	96.56	96.93
9	50 (−1)	9 (−1)	35 (−1)	90 (+1)	67.22	68.4
10	70 (+1)	9 (−1)	35 (−1)	90 (+1)	93.33	91.84
11	50 (−1)	11 (+1)	35 (−1)	90 (+1)	90.51	90.14
12	70 (+1)	11 (+1)	35 (−1)	90 (+1)	95.87	96.85
13	50 (−1)	9 (−1)	55 (+1)	90 (+1)	78.95	77.6
14	70 (+1)	9 (−1)	55 (+1)	90 (+1)	96.87	97.91
15	50 (−1)	11 (+1)	55 (+1)	90 (+1)	94.02	94.87

Table 3. Cont.

S. N	Independent Parameters <sup>(1)</sup>				Response (Y): NH <sub>3</sub> -N Removal Efficiency (%)	
	A (°C)	B	C (kPa)	D (Min)	Experimental Value	Predicted Value
16	70 (+1)	11 (+1)	55 (+1)	90 (+1)	99.25	98.44
17	50 (−1)	10 (0)	45 (0)	75 (0)	84.54	85.05
18	70 (+1)	10 (0)	45 (0)	75 (0)	97.07	98.75
19	60 (0)	9 (−1)	45 (0)	75(0)	74.89	77.25
20	60 (0)	11 (+1)	45(0)	75 (0)	91.14	90.96
21	60 (0)	10 (0)	35 (−1)	75 (+1)	85.31	85.83
22	60 (0)	10 (0)	55 (+1)	75 (+1)	91.00	92.66
23	60 (0)	10 (0)	45 (0)	60 (0)	84.61	86.82
24	60 (0)	10 (0)	45 (0)	90 (+1)	92.56	92.53
25	60 (0)	10 (0)	45 (0)	75 (0)	91.04	89.43
26	60 (0)	10 (0)	45 (0)	75 (0)	90.55	89.43
27	60 (0)	10 (0)	45 (0)	75 (0)	89.22	89.43
28	60 (0)	10 (0)	45 (0)	75 (0)	88.79	89.43
29	60 (0)	10 (0)	45 (0)	75 (0)	92.02	89.43
30	60 (0)	10 (0)	45 (0)	75 (0)	91.5	89.43

<sup>(1)</sup> A: temperature (°C), B: pH, C: vacuum pressure (kPa), D: treatment time (min).

The ANOVA results for the quadratic model of NH<sub>3</sub>-N removal are shown in Table 4.

Table 4. ANOVA results for the response surface quadratic model.

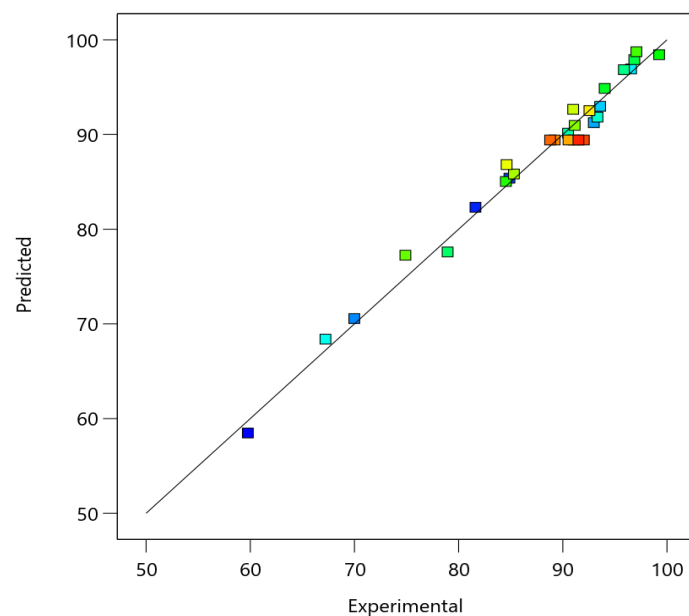
Scheme	Sum of Squares	df <sup>a</sup>	Mean Square	F-Value	p-Value	Remarks
Model	2501.51	14	178.68	56.19	<0.0001	*
A (Temperature)	844.60	1	844.60	265.62	<0.0001	*
B (pH)	846.25	1	846.25	266.14	<0.0001	*
C (Vacuum Pressure)	209.99	1	209.99	66.04	<0.0001	*
D (Treatment Time)	146.55	1	146.55	46.09	<0.0001	*
AB	280.31	1	280.31	88.16	<0.0001	*
AC	9.84	1	9.84	3.10	0.0989	**
AD	0.1463	1	0.1463	0.0460	0.8330	**
BC	20.05	1	20.05	6.31	0.0240	*
BD	26.55	1	26.55	8.35	0.0112	*
CD	8.22	1	8.22	2.59	0.1287	**
A <sup>2</sup>	15.83	1	15.83	4.98	0.0414	*
B <sup>2</sup>	73.29	1	73.29	23.05	0.0002	*
C <sup>2</sup>	0.0826	1	0.0826	0.0260	0.8741	**
D <sup>2</sup>	0.1639	1	0.1639	0.0515	0.8235	**
Residual	47.70	15	3.18			
Lack of Fit	39.53	10	3.95	2.42	0.1706	**
Pure Error	8.16	5	1.63			
R <sup>2</sup>	0.98					
Adjusted R <sup>2</sup>	0.96					
Predicted R <sup>2</sup>	0.92					
Adequate precision	31.93					

<sup>a</sup> df: Degree of freedom. \* Significant. \*\* Not significant.

In RSM, the model parameters, including Fisher's F-value, lack of fit, and adequate precision, play a crucial role in illustrating the developed model's significance, competency, and soundness [33]. The model's F-value of 56.19, with a p-value < 0.0001, indicated that the constructed model was highly significant at a 95% confidence level. This suggested that the regression model could reliably predict NH<sub>3</sub>-N removal efficiency. The lack of fit value compares the residual error to pure error for an experimental design, and it should be insignificant to validate the authenticity of the developed model [34]. The non-

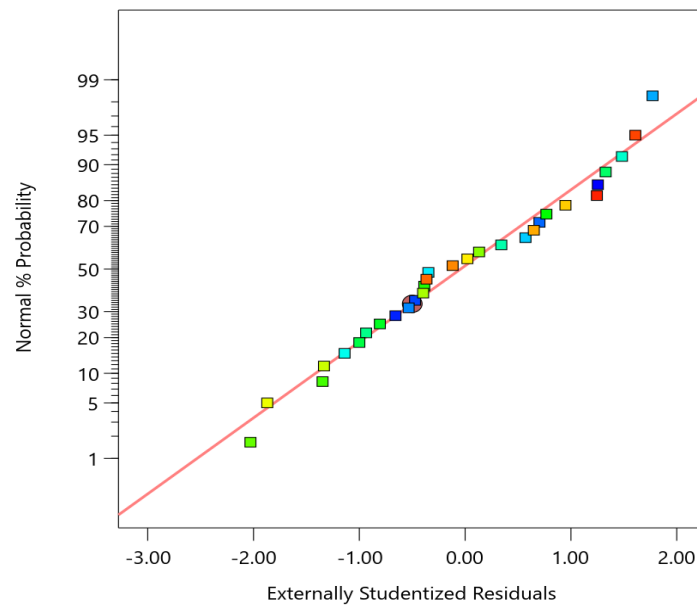
significant ( $p > 0.05$ ) lack of fit relative to pure error indicated the validity of the quadratic models [35]. Adequate precision evaluates the signal-to-noise ratio by comparing the predicted value ranges to the mean prediction error at the design points. Ratios above 4 are preferable [36]. In this study, a high adequate precision value of 31.93 was observed, indicating the adequacy of the developed model. Furthermore, high  $R^2$  values between the observed and predicted values for  $\text{NH}_3\text{-N}$  removal elucidated the goodness of fit and statistical significance of the model. In this study, both the  $R^2$  adj (0.96) and  $R^2$  pre (0.92) values were obtained from the Design-Expert<sup>®</sup> software version 13.0.5 and found to be in good agreement. Since the value of  $R^2 > 0.8$ , there was a good agreement between the observed and predicted values. The empirical models closely fit the experimental data when the  $R^2$  value is close to unity (1.0) [37].

The data fitting potential of the developed RSM model was tested by plotting the predicted values against experimental data for  $\text{NH}_3\text{-N}$  removal (Figure 1). The experimental values, which were symmetrically distributed, were very close to the predicted data, showing good agreement between the experimental and predicted values for  $\text{NH}_3\text{-N}$  removal from RLDM. Each data point aligned precisely with or very near to the line of fitness, providing additional evidence for the high  $R^2$  value attained by this model. Since these values were very close to a perfect fit, a good agreement between the predicted values and the experimental values of the model was achieved [38].



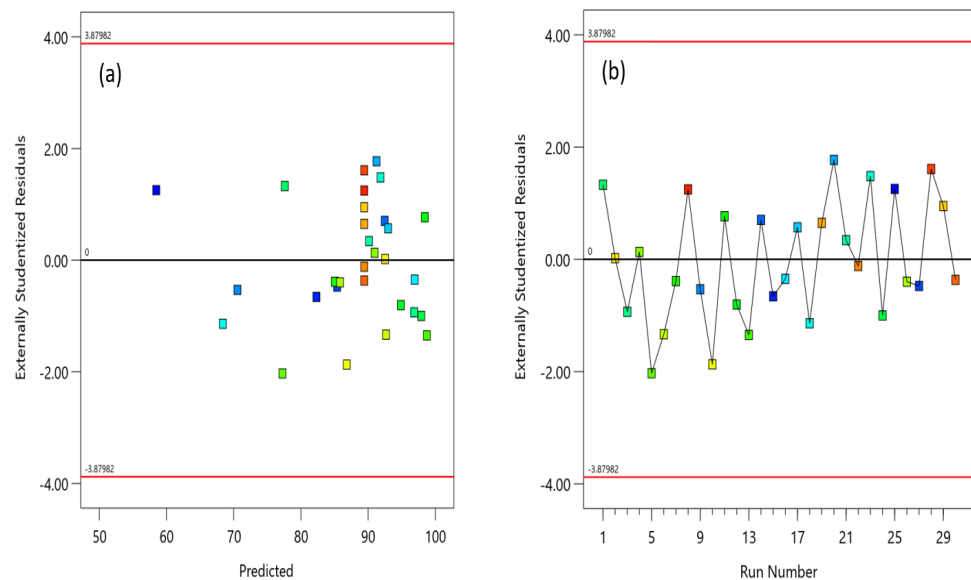
**Figure 1.** Linear fit for predicted versus experimental  $\text{NH}_3\text{-N}$  removal from RLDM.

The differences between the numbers obtained from the experiment and those fitted by the model are residuals [39]. Analysis of residuals is necessary to confirm that the assumptions for the ANOVA are met. Diagnostic plots of residuals were produced and evaluated to ensure that this model approximated the real system adequately [34]. Figure 2 presents the normal probability plot of standardized residual. It shows a reasonably good fit of the normal probability percentage versus standardized residuals, representing that the model prediction statistically fits the observed results. The points resulting from the test should be positioned in a straight line to indicate the normality of the data [39]. The points are approximately along a straight line; thus, it can be inferred that the residuals have a normal distribution.



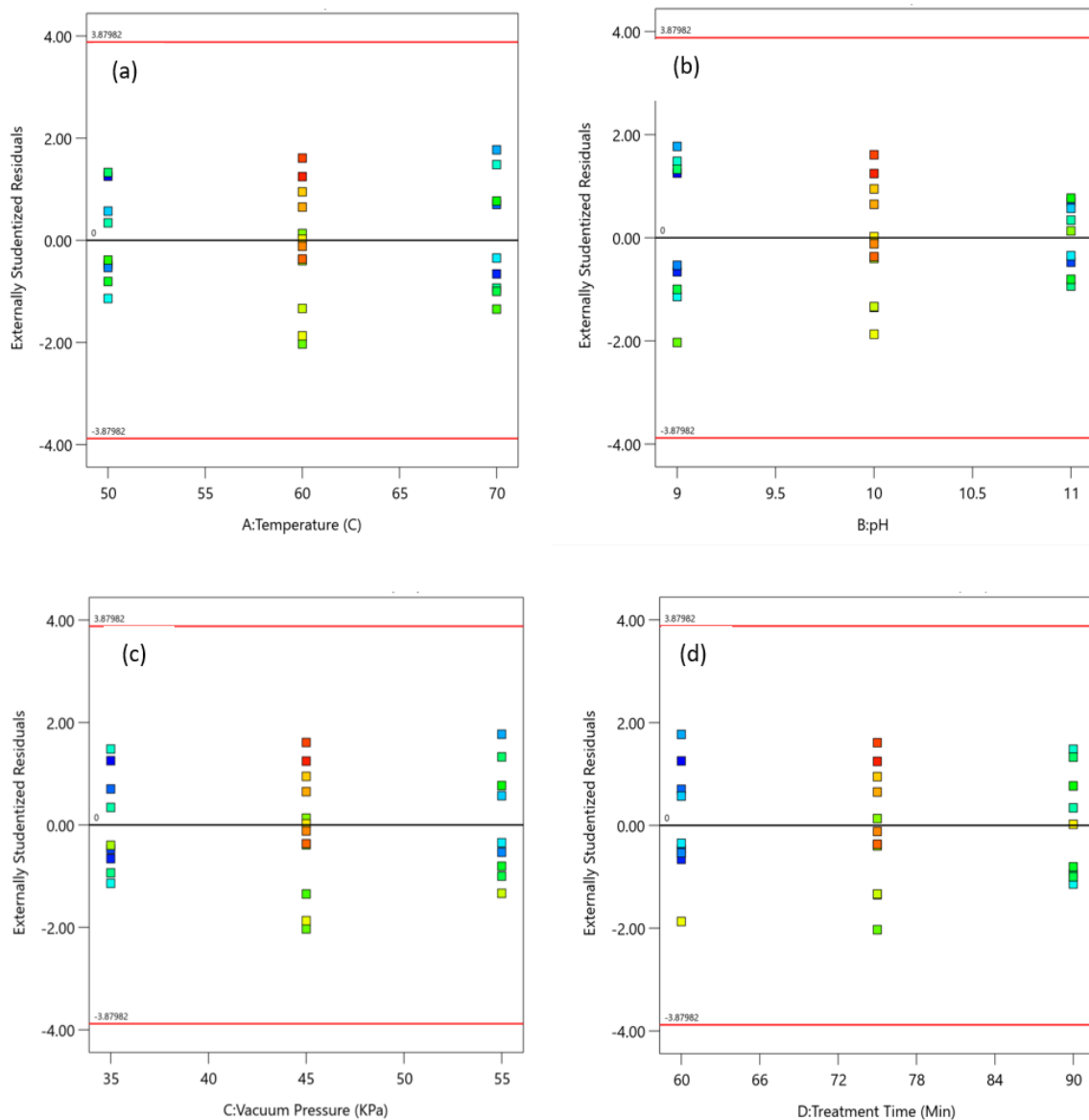
**Figure 2.** Normal probability plot of externally studentized residuals for  $\text{NH}_3\text{-N}$  removal from RLDM.

Figure 3a,b are standardized residual versus predicted and run values, respectively. It is evident that neither plot showed any obvious patterns. The student residual changes versus predicted values are presented in Figure 3a. As can be observed, the points in this figure follow a specific random scattering pattern, indicating that the points must be distributed randomly. Figure 3b shows the graph of the residuals versus the run numbers. None of the data are outside of the standard deviation range, demonstrating the data's random distribution.



**Figure 3.** Diagnostics plots for  $\text{NH}_3\text{-N}$  removal from RLDM externally studentized residual versus (a) predicted values, (b) experimental values.

The diagnostic plots (Figure 4a–d) depicting externally studentized residuals against the studied parameters (temperature, pH, vacuum pressure, treatment time) revealed no outliers. Since there were no outliers, the models suggest the reliability of the dataset [34].



**Figure 4.** Diagnostics plots for  $\text{NH}_3\text{-N}$  removal from RLDM externally studentized residual versus (a) temperature ( $^{\circ}\text{C}$ ), (b) pH, (c) vacuum pressure (kPa), (d) treatment time (min).

### 3.2. Impact of Operational Variables on Process Performance

The 3D surface and 2D contour plots represent the regression equation for optimizing reaction conditions. Response surface methodology (RSM) contour plots indicate the relationship between two factors while maintaining all other variables constant, usually at the zero level [40]. Figure 5 illustrates the 3D response surface plots for all variables (AB, BC, BD, AC, AD, and CD) plotted against the response. Response surface plots in three dimensions are essentially like contour plots but come with an embedded response surface.

Considering the interactive association of the selected parameters, the collaborative impact of temperature (A) and pH (B), pH (B) and vacuum pressure (C), and pH (B) and treatment time (D) were found to be significant. As depicted in Figure 5a, the temperature range of 57–70  $^{\circ}\text{C}$  and a pH greater than 9.5 defined the region of maximum response, achieving a conversion of  $\geq 95\%$ . Similarly, Figure 5b illustrates that a vacuum pressure of 40–55 kPa and a pH of  $\geq 9.5$  resulted in a conversion of  $\geq 90\%$ . Additionally, Figure 5c showed that a treatment time within the 65–90 min range and a pH between 9.5 and 11 consistently led to a conversion of  $\geq 90\%$ . The former factors (A and B) demonstrated a

more prominent impact, as reflected in their higher F-values. No significant interactions were found between AC, CD, and AD for NH<sub>3</sub>-N removal ( $p > 0.05$ ).

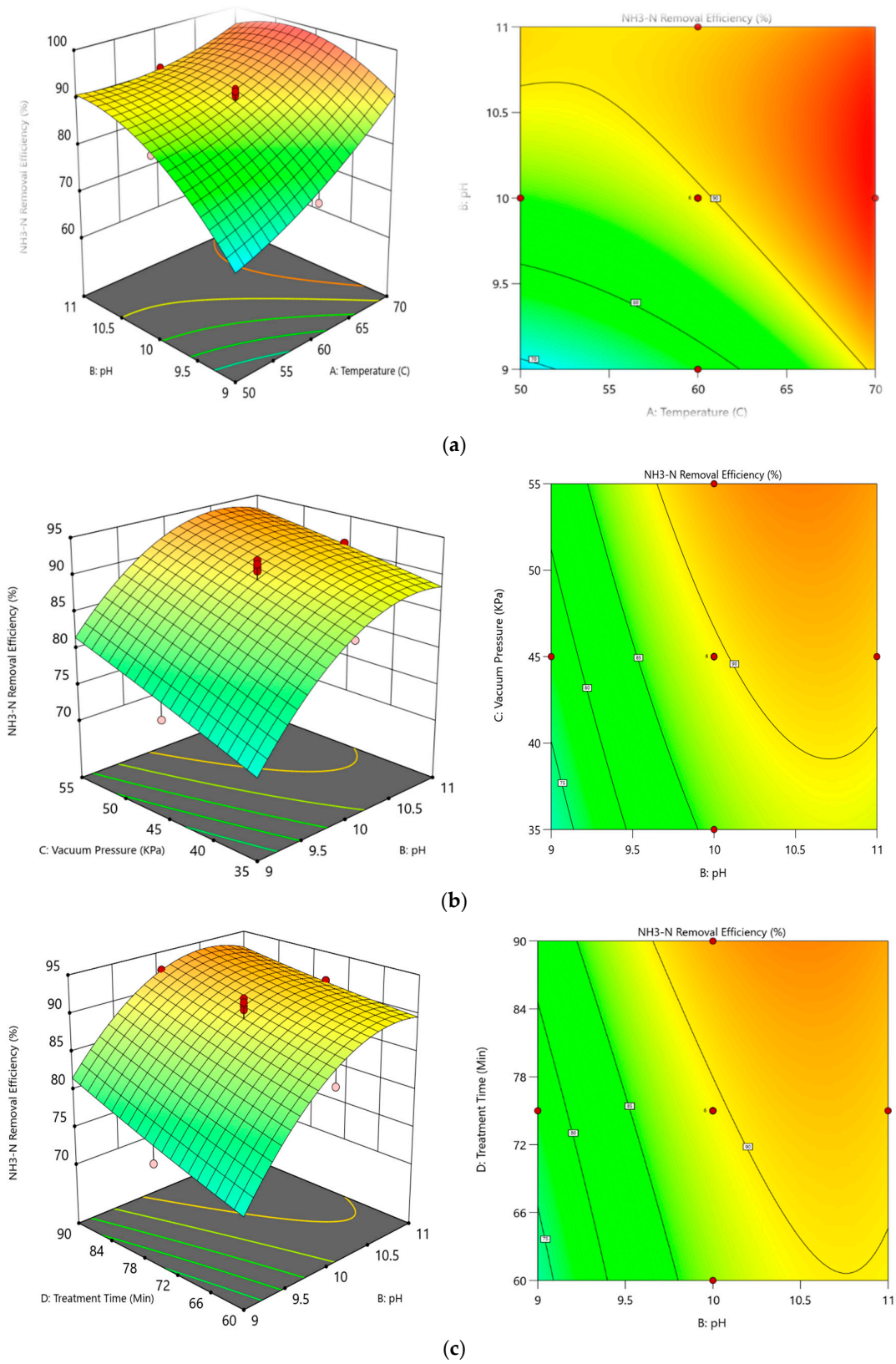
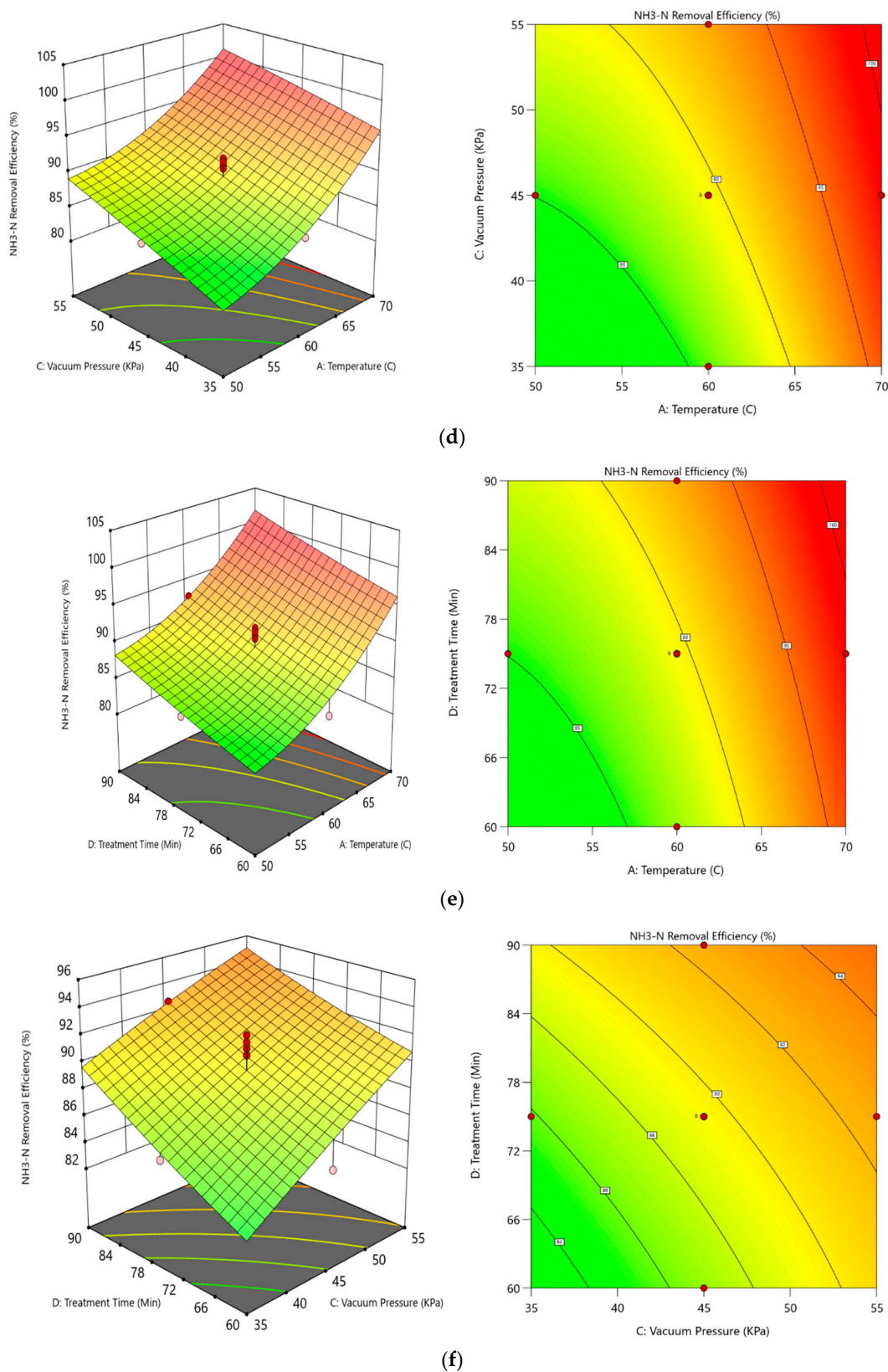


Figure 5. Cont.



**Figure 5.** Three- and two-dimensional contour plots for NH<sub>3</sub>-N removal from RLDM: (a) temperature (°C) × pH, (b) pH × vacuum pressure, (c) pH × treatment time (min), (d) temperature (°C) × vacuum pressure, (e) temperature (°C) × treatment time (min), (f) vacuum pressure × treatment time (min).

Enhanced NH<sub>3</sub>-N removal efficiency was associated with increased temperature, pH, vacuum pressure, and treatment time. The role of pH was particularly influential, resulting in a significant rise in NH<sub>3</sub>-N removal efficiency, as depicted in Figure 5a–c. Ammonium (NH<sub>4</sub><sup>+</sup>) represents the non-volatile state of NH<sub>3</sub>. A higher pH causes more ammonium ions to be converted to ammonia. This transformation is caused by the interaction between pH and the ionization of weak acids (NH<sub>4</sub><sup>+</sup>). A study by Gustin and Marinšek-Logar [31] examined the effects of pH, temperature, and airflow on the recovery of NH<sub>3</sub> from anaerobically digested wastewater. The findings indicated that stripping was most significantly affected by a high pH that changed the NH<sub>3</sub> to NH<sub>4</sub><sup>+</sup> ratio in favor of NH<sub>3</sub> accumulation. Similarly, Chen et al. [21] investigated vacuum ammonia stripping on liquid digestate in which adjusting the initial pH above 9.5 and maintaining alkalinity led to over 80% NH<sub>3</sub>-N removal efficiency during a 30 min vacuum stripping process. pH and alkalinity emerged as primary factors for ammonia nitrogen dissociation and removal, while temperature and vacuum played key roles in enhancing ammonia nitrogen mass transfer and removal speed [21]. While higher pH values are generally more favorable for NH<sub>3</sub>-N removal, there is an optimal pH range that balances efficient NH<sub>3</sub> removal with practical considerations. The overall efficiency of the process may not benefit from pH values that are too high or too low. Moreover, the efficiency of the stripping process is frequently influenced by temperature. Higher temperatures can potentially accelerate the conversion of NH<sub>4</sub><sup>+</sup> to NH<sub>3</sub> [41]. Therefore, the combination of higher pH and temperature can collaboratively enhance the NH<sub>3</sub> volatilization.

### 3.3. Optimization of the Process Parameters

The numerical optimization tool utilizing the desirability function was used to maximize the response. The target response (NH<sub>3</sub>-N removal) and independent operational variables in this study were set at “maximum” and “within the range”, respectively, as the preferred levels. All factors were assigned equal weightage (+++), and the proposed experimental setup for optimal performance (desirability = 1) was determined at a temperature of 69.9 °C, pH of 10.5, vacuum pressure of 53.5 kPa, and treatment time of 64.2 min. Three tests were performed under optimized conditions to validate the model’s predictive potential. As can be seen from Table 5, there is a substantial agreement between the experimental and predictive values at the optimal levels, indicating a high degree of model validity.

**Table 5.** Predicted and experimental values under optimum conditions for model validation.

Parameters <sup>(1)</sup>	Optimum Conditions	Response (NH <sub>3</sub> -N Removal Efficiency (%))			
		Predicted Value	Experimental Value	95% CI Low	95% CI High
A	69.9				
B	10.5				
C	53.5	99.29	98.58 ± 1.05	96.76	101.83
D	64.2				

<sup>(1)</sup> A: temperature (°C), B: pH, C: vacuum pressure (kPa), D: treatment time (min).

Furthermore, as established by graphic optimization, the region of possible response values in the factor space is shown in a graphic overlay plot of the contour graphs. Figure 6 indicates the graphical optimization at temperature (50–70 min) and pH (9–11). The shaded region depicted in the overlay plot represents the area that satisfies the proposed criteria [42]. The shaded yellow area designates the optimum zone, providing a focused design space [20]. The chosen value for NH<sub>3</sub>-N removal was 99.91%, achieved at the temperature, pH, vacuum pressure, and treatment time of 69.7 °C, 9.7, 51.2 kPa, and 75 min, respectively. This specific point is marked with a flag.

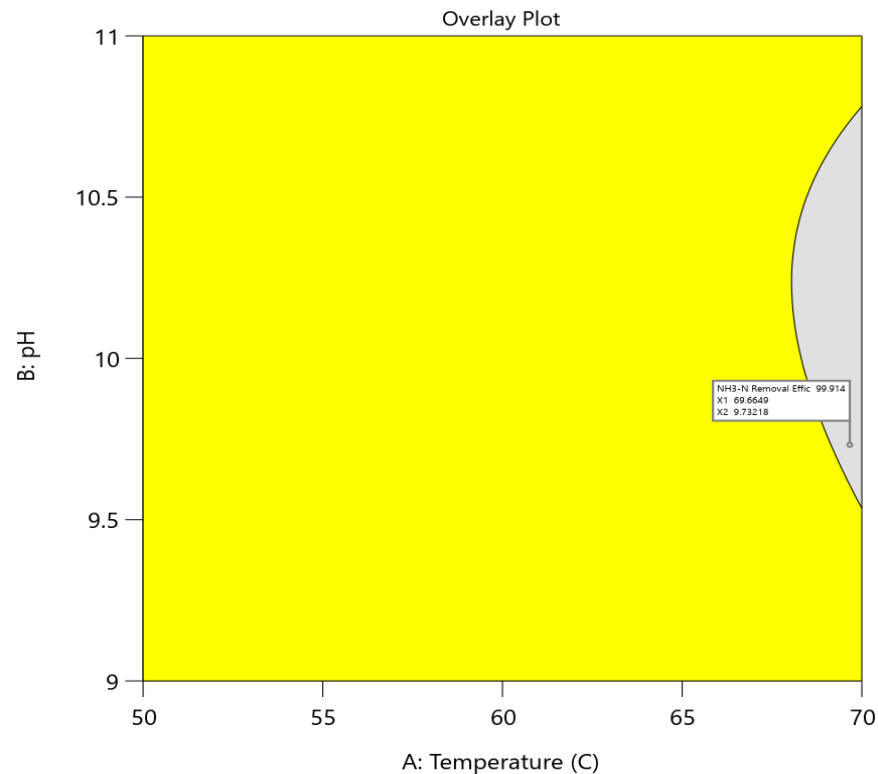
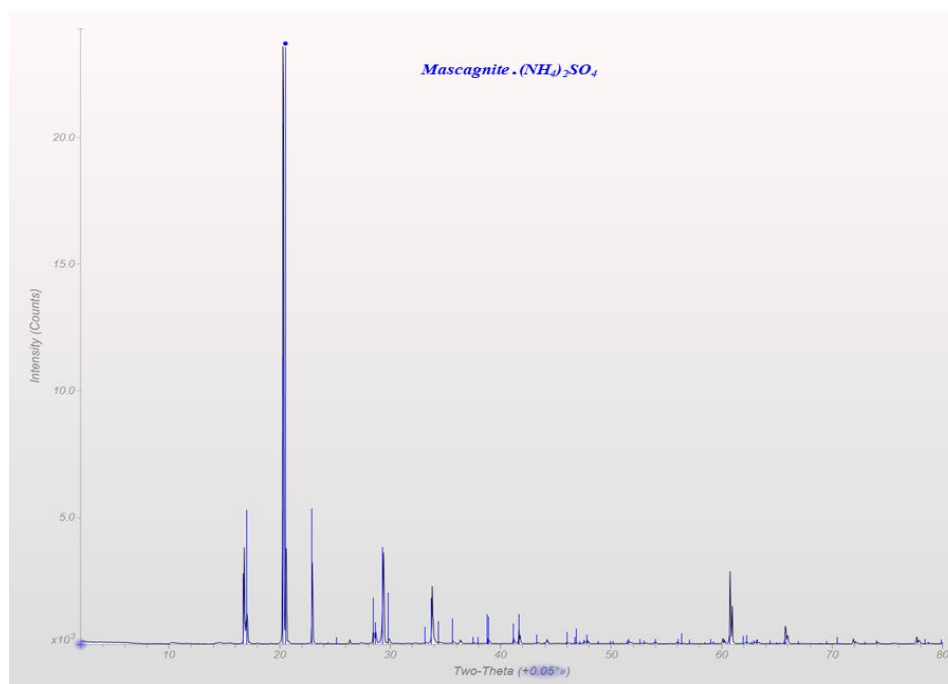


**Figure 6.** Overlay plot showing the optimal region.

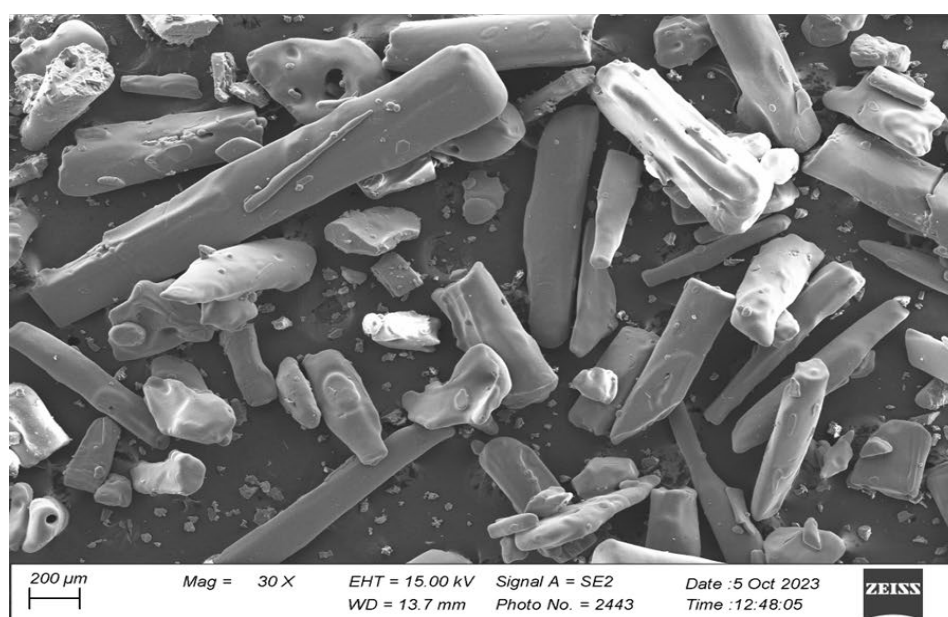
### 3.4. Ammonia Nitrogen Recovery

The structure and morphology of the recovered ammonium sulfate ( $(\text{NH}_4)_2\text{SO}_4$ ) from RDLM under the optimal conditions was determined by X-ray diffraction (XRD) and scanning electron microscopy (SEM) analyses. The XRD analysis revealed that the  $\text{NH}_3\text{-N}$  stripped during the VTS-AA was recovered as  $(\text{NH}_4)_2\text{SO}_4$  (Muscagnite) (Figure 7a). According to the XRD analysis, the position and intensity of the recovered  $(\text{NH}_4)_2\text{SO}_4$  matched those of the commercial product. The findings from X-ray diffraction analysis, illustrated in Figure 7a, established the nature of the precipitate as Muscagnite, an ammonium sulfate mineral, characterized by its orthorhombic crystalline structure, as evidenced by the consistency in peak intensity and positions with the established pattern typical of orthorhombic ammonium sulfate crystals. Through X-ray diffraction (XRD), coherent scattering of X-rays leads to constructive interference, giving rise to diffraction peaks that reflect the atomic plane spacing and the wavelength of the X-rays utilized [43]. High purity  $(\text{NH}_4)_2\text{SO}_4$  crystals (~98%) can be obtained by absorption of  $\text{NH}_3\text{-N}$  in a  $\text{H}_2\text{SO}_4$  solution pre-saturated with  $(\text{NH}_4)_2\text{SO}_4$  and cooling, ultimately leading to a product that can be sold as a fertilizer or an analytical grade granular chemical [41].

SEM was used to perform qualitative analysis and physical morphology of the experimental  $(\text{NH}_4)_2\text{SO}_4$  crystals. Figure 7b represents the orthorhombic, irregular, and uneven crystal structures of the recovered  $(\text{NH}_4)_2\text{SO}_4$ . The structure of the form complied with the findings in the literature [20,41].



(a)



(b)

**Figure 7.** Recovered  $(\text{NH}_4)_2\text{SO}_4$  crystals (a) XRD and (b) SEM images.

#### 4. Conclusions

This study optimized the VTS-AA process to remove and recover  $\text{NH}_3\text{-N}$  from RLDM using an RSM-based CCD approach. Through this optimization technique, the ideal conditions for VTS-AA process for  $\text{NH}_3\text{-N}$  removal and recovery from RLDM were determined, highlighting the model's reliability. The ANOVA analysis revealed the influence of operational factors on  $\text{NH}_3\text{-N}$  removal from RLDM. The optimal values of temperature, pH, vacuum pressure, and treatment time were found to be 69.9  $^\circ\text{C}$ , 10.5, 53.5 kPa, and 64.2 min, respectively, resulting in an  $\text{NH}_3\text{-N}$  removal efficiency of 98.58% in experimental trials. The RSM model predicted value aligned well with the experimentally obtained  $\text{NH}_3\text{-N}$  removal

value. Similarly, the recovered  $(\text{NH}_4)_2\text{SO}_4$  was confirmed and validated as  $(\text{NH}_4)_2\text{SO}_4$  crystals from XRD and SEM analysis results. To sum up, this study provides a valuable reference for raw dairy manure treatment, offering a multi-step process with promising industrial applications and a sustainable approach to nutrient recycling.

## 5. Future Remarks

This study relies mainly on experimental datasets from laboratory analyses and pilot-scale tests [19,20,25]. Future research should aim to conduct industrial-scale trials to evaluate the practical and economic viability of the VTS-AA technology. Additionally, it is integral to incorporate cost–benefit analysis to assess the economic feasibility and competitiveness of this technology compared to conventional waste management practices. Although current research has primarily focused on optimizing processes, a thorough investigation of recovery rates and yields could lead to significant advancements in sustainable resource management. Despite existing challenges, these findings serve as a key reference, aiding in the advancement and application of VTS-AA treatment technology for sustainable raw dairy manure management.

**Author Contributions:** Conceptualization, S.S. and L.C.; methodology, S.S., A.R. and L.C.; software, S.S.; validation, L.C., S.S. and A.R.; formal analysis, S.S.; investigation, S.S.; resources, L.C.; data curation, S.S., A.R. and L.C.; writing—original draft preparation, S.S.; writing—review and editing, S.S., L.C. and A.R.; visualization, S.S.; supervision, L.C.; project administration, L.C.; funding acquisition, L.C. All authors have read and agreed to the published version of the manuscript.

**Funding:** The work was funded by the USDA National Institute of Food and Agriculture (NIFA), the Hatch Project (Project No. IDA011745, Accession No. 7006606), and the USDA NIFA Sustainable Agricultural Systems project (Award No. 2020-69012-31871).

**Data Availability Statement:** The original contributions presented in the study are included in the article, further inquiries can be directed to the corresponding author/s.

**Conflicts of Interest:** The authors confirm that there are no conflicts of interest to report.

## References

1. U.S. Environmental Protection Agency. National Emission Inventory—Ammonia Emissions from Animal Husbandry Operations. 2004. Available online: [https://www3.epa.gov/ttnchie1/ap42/ch09/related/nh3inventorydraft\\_jan2004.pdf](https://www3.epa.gov/ttnchie1/ap42/ch09/related/nh3inventorydraft_jan2004.pdf) (accessed on 29 April 2024).
2. Zhang, H.; Schroder, J. Animal Manure Production and Utilization in the US. In *Applied Manure and Nutrient Chemistry for Sustainable Agriculture and Environment*; He, Z., Zhang, H., Eds.; Springer: Dordrecht, The Netherlands, 2014; pp. 1–21. [CrossRef]
3. Sarkar, B.; Chakrabarti, P.P.; Vijaykumar, A.; Kale, V. Wastewater Treatment in Dairy Industries—Possibility of Reuse. *Desalination* **2006**, *195*, 141–152. [CrossRef]
4. Hubbard, R.; Lowrance, R. Management of Dairy Cattle Manure. *Agric. Uses Munic. Anim. Ind. Byprod.* **1998**, *5*, 91–102.
5. Thomas Ukwuani, A.; Tao, W.; Han, J. *Ammonia Recovery from Dairy Manure*; ASABE Paper No. 131590424; ASABE: St. Joseph, MI, USA, 2013; p. 1. [CrossRef]
6. Agyeman, F.O.; Tao, W. Anaerobic Co-Digestion of Food Waste and Dairy Manure: Effects of Food Waste Particle Size and Organic Loading Rate. *J. Environ. Manag.* **2014**, *133*, 268–274. [CrossRef]
7. Chen, T.-L.; Chen, L.-H.; Lin, Y.J.; Yu, C.-P.; Ma, H.; Chiang, P.-C. Advanced Ammonia Nitrogen Removal and Recovery Technology Using Electrokinetic and Stripping Process towards a Sustainable Nitrogen Cycle: A Review. *J. Clean. Prod.* **2021**, *309*, 127369. [CrossRef]
8. Kumar, R.; Pal, P. Assessing the Feasibility of N and P Recovery by Struvite Precipitation from Nutrient-Rich Wastewater: A Review. *Environ. Sci. Pollut. Res.* **2015**, *22*, 17453–17464. [CrossRef]
9. Jiang, A.; Zhang, T.; Zhao, Q.-B.; Li, X.; Chen, S.; Frear, C.S. Evaluation of an Integrated Ammonia Stripping, Recovery, and Biogas Scrubbing System for Use with Anaerobically Digested Dairy Manure. *Biosyst. Eng.* **2014**, *119*, 117–126. [CrossRef]
10. Yellezuome, D.; Zhu, X.; Wang, Z.; Liu, R. Mitigation of Ammonia Inhibition in Anaerobic Digestion of Nitrogen-Rich Substrates for Biogas Production by Ammonia Stripping: A Review. *Renew. Sustain. Energy Rev.* **2022**, *157*, 112043. [CrossRef]
11. Ledda, C.; Schievano, A.; Salati, S.; Adani, F. Nitrogen and Water Recovery from Animal Slurries by a New Integrated Ultrafiltration, Reverse Osmosis and Cold Stripping Process: A Case Study. *Water Res.* **2013**, *47*, 6157–6166. [CrossRef] [PubMed]
12. Zeng, L.; Mangan, C.; Li, X. Ammonia Recovery from Anaerobically Digested Cattle Manure by Steam Stripping. *Water Sci. Technol.* **2006**, *54*, 137–145. [CrossRef] [PubMed]

13. Uludag-Demirer, S.; Demirer, G.N.; Frear, C.; Chen, S. Anaerobic Digestion of Dairy Manure with Enhanced Ammonia Removal. *J. Environ. Manag.* **2008**, *86*, 193–200. [CrossRef]
14. Zeng, L.; Li, X. Nutrient Removal from Anaerobically Digested Cattle Manure by Struvite Precipitation. *J. Environ. Eng. Sci.* **2006**, *5*, 285–294. [CrossRef]
15. Zarebska, A.; Nieto, D.R.; Christensen, K.V.; Norddahl, B. Ammonia Recovery from Agricultural Wastes by Membrane Distillation: Fouling Characterization and Mechanism. *Water Res.* **2014**, *56*, 1–10. [CrossRef] [PubMed]
16. Palakodeti, A.; Azman, S.; Rossi, B.; Dewil, R.; Appels, L. A Critical Review of Ammonia Recovery from Anaerobic Digestate of Organic Wastes via Stripping. *Renew. Sustain. Energy Rev.* **2021**, *143*, 110903. [CrossRef]
17. Robles, Á.; Aguado, D.; Barat, R.; Borrás, L.; Bouzas, A.; Giménez, J.B.; Martí, N.; Ribes, J.; Ruano, M.V.; Serralta, J.; et al. New Frontiers from Removal to Recycling of Nitrogen and Phosphorus from Wastewater in the Circular Economy. *Bioresour. Technol.* **2020**, *300*, 122673. [CrossRef]
18. Hegemann, M.H.; Warnecke, H.-J.; Viljoen, H.J. Removal of Ammonia from Aqueous Systems in a Semibatch Reactor. *Ind. Eng. Chem. Res.* **2001**, *40*, 3361–3368. [CrossRef]
19. Ukwuani, A.T.; Tao, W. Developing a Vacuum Thermal Stripping—Acid Absorption Process for Ammonia Recovery from Anaerobic Digester Effluent. *Water Res.* **2016**, *106*, 108–115. [CrossRef]
20. Reza, A.; Chen, L. Optimization and Modeling of Ammonia Nitrogen Removal from Anaerobically Digested Liquid Dairy Manure Using Vacuum Thermal Stripping Process. *Sci. Total Environ.* **2022**, *851*, 158321. [CrossRef]
21. Chen, Q.; Yang, D.; Chen, X.; Wang, X.; Dong, B.; Dai, X. Vacuum Ammonia Stripping from Liquid Digestate: Effects of pH, Alkalinity, Temperature, Negative Pressure and Process Optimization. *J. Environ. Sci.* **2025**, *149*, 638–650. [CrossRef]
22. Tao, W.; Bayrakdar, A.; Wang, Y.; Agyeman, F. Three-Stage Treatment for Nitrogen and Phosphorus Recovery from Human Urine: Hydrolysis, Precipitation and Vacuum Stripping. *J. Environ. Manag.* **2019**, *249*, 109435. [CrossRef] [PubMed]
23. Zhang, R. Development of an Innovative Thermal-Vacuum Stripping Assisted Thermophilic Anaerobic Digestion Process and System for Complete Utilization of Liquid Swine Manure. Ph.D. Thesis, University of Minnesota, Minneapolis, MN, USA, 2021. Available online: <https://www.proquest.com/docview/2502671310/abstract/8B6E6DBE61094486PQ/1> (accessed on 12 November 2023).
24. Dawson, C.J.; Hilton, J. Fertiliser Availability in a Resource-Limited World: Production and Recycling of Nitrogen and Phosphorus. *Food Policy* **2011**, *36*, S14–S22. [CrossRef]
25. Han, Y.; Agyeman, F.; Green, H.; Tao, W. Stable, High-Rate Anaerobic Digestion through Vacuum Stripping of Digestate. *Bioresour. Technol.* **2022**, *343*, 126133. [CrossRef] [PubMed]
26. Rongwong, W.; Sairiam, S. A Modeling Study on the Effects of pH and Partial Wetting on the Removal of Ammonia Nitrogen from Wastewater by Membrane Contactors. *J. Environ. Chem. Eng.* **2020**, *8*, 104240. [CrossRef]
27. Mohammed-Nour, A.; Al-Sewailem, M.; El-Naggar, A.H. The Influence of Alkalization and Temperature on Ammonia Recovery from Cow Manure and the Chemical Properties of the Effluents. *Sustainability* **2019**, *11*, 2441. [CrossRef]
28. EL-Bourawi, M.S.; Khayet, M.; Ma, R.; Ding, Z.; Li, Z.; Zhang, X. Application of Vacuum Membrane Distillation for Ammonia Removal. *J. Membr. Sci.* **2007**, *301*, 200–209. [CrossRef]
29. Hameed, B.H.; Tan, I.A.W.; Ahmad, A.L. Optimization of Basic Dye Removal by Oil Palm Fibre-Based Activated Carbon Using Response Surface Methodology. *J. Hazard. Mater.* **2008**, *158*, 324–332. [CrossRef]
30. Shim, S.; Won, S.; Reza, A.; Kim, S.; Ahmed, N.; Ra, C. Design and Optimization of Fluidized Bed Reactor Operating Conditions for Struvite Recovery Process from Swine Wastewater. *Processes* **2020**, *8*, 422. [CrossRef]
31. Guštin, S.; Marinšek-Logar, R. Effect of pH, Temperature and Air Flow Rate on the Continuous Ammonia Stripping of the Anaerobic Digestion Effluent. *Process Saf. Environ. Prot.* **2011**, *89*, 61–66. [CrossRef]
32. Kumar, R.; Pal, P. Turning Hazardous Waste into Value-Added Products: Production and Characterization of Struvite from Ammoniacal Waste with New Approaches. *J. Clean. Prod.* **2013**, *43*, 59–70. [CrossRef]
33. Bashir, M.J.K.; Aziz, H.A.; Yusoff, M.S.; Adlan, M.N. Application of Response Surface Methodology (RSM) for Optimization of Ammoniacal Nitrogen Removal from Semi-Aerobic Landfill Leachate Using Ion Exchange Resin. *Desalination* **2010**, *254*, 154–161. [CrossRef]
34. Ding, Y.; Sartaj, M. Statistical Analysis and Optimization of Ammonia Removal from Aqueous Solution by Zeolite Using Factorial Design and Response Surface Methodology. *J. Environ. Chem. Eng.* **2015**, *3*, 807–814. [CrossRef]
35. Mehmood, T.; Ahmed, A.; Ahmad, A.; Ahmad, M.S.; Sandhu, M.A. Optimization of Mixed Surfactants-Based  $\beta$ -Carotene Nanoemulsions Using Response Surface Methodology: An Ultrasonic Homogenization Approach. *Food Chem.* **2018**, *253*, 179–184. [CrossRef]
36. Bilici Baskan, M.; Pala, A. A Statistical Experiment Design Approach for Arsenic Removal by Coagulation Process Using Aluminum Sulfate. *Desalination* **2010**, *254*, 42–48. [CrossRef]
37. Taufiqurrahmi, N.; Mohamed, A.R.; Bhatia, S. Production of Biofuel from Waste Cooking Palm Oil Using Nanocrystalline Zeolite as Catalyst: Process Optimization Studies. *Bioresour. Technol.* **2011**, *102*, 10686–10694. [CrossRef] [PubMed]
38. Krishnamurthy, K.N.; Sridhara, S.N.; Ananda Kumar, C.S. Optimization and Kinetic Study of Biodiesel Production from *Hydnocarpus Wightiana* Oil and Dairy Waste Scum Using Snail Shell CaO Nano Catalyst. *Renew. Energy* **2020**, *146*, 280–296. [CrossRef]

39. Dargahi, A.; Samarghandi, M.R.; Shabanloo, A.; Mahmoudi, M.M.; Nasab, H.Z. Statistical Modeling of Phenolic Compounds Adsorption onto Low-Cost Adsorbent Prepared from Aloe Vera Leaves Wastes Using CCD-RSM Optimization: Effect of Parameters, Isotherm, and Kinetic Studies. *Biomass Conv. Bioref.* **2023**, *13*, 7859–7873. [[CrossRef](#)]
40. Ahmad, A.L.; Ismail, S.; Bhatia, S. Optimization of Coagulation–Flocculation Process for Palm Oil Mill Effluent Using Response Surface Methodology. *Environ. Sci. Technol.* **2005**, *39*, 2828–2834. [[CrossRef](#)] [[PubMed](#)]
41. Tao, W.; Ukwuani, A.T. Coupling Thermal Stripping and Acid Absorption for Ammonia Recovery from Dairy Manure: Ammonia Volatilization Kinetics and Effects of Temperature, pH and Dissolved Solids Content. *Chem. Eng. J.* **2015**, *280*, 188–196. [[CrossRef](#)]
42. Zinatizadeh, A.a.L.; Mansouri, Y.; Akhbari, A.; Pashaei, S. Biological Treatment of a Synthetic Dairy Wastewater in a Sequencing Batch Biofilm Reactor: Statistical Modeling Using Optimization Using Response Surface Methodology. *Chem. Ind. Chem. Eng. Q.* **2011**, *17*, 485–495. [[CrossRef](#)]
43. Amonette, J.E. Methods for Determination of Mineralogy and Environmental Availability. In *Soil Mineralogy with Environmental Applications*; John Wiley & Sons, Ltd.: Hoboken, NJ, USA, 2002; pp. 153–197. [[CrossRef](#)]

**Disclaimer/Publisher’s Note:** The statements, opinions and data contained in all publications are solely those of the individual author(s) and contributor(s) and not of MDPI and/or the editor(s). MDPI and/or the editor(s) disclaim responsibility for any injury to people or property resulting from any ideas, methods, instructions or products referred to in the content.